Pergamon

0301-9322(95)00033-X

Int. J. Multiphase Flow Vol. 21, No. 6, pp. 1191–1201, 1995

0301-9322/95 $9.50 + 0.00

DISENGAGEMENT OF THE GAS PHASE IN BUBBLE COLUMNS

N. S. DESHPANDE, M. DINKAR and J. B. JOSHI†
Department of Chemical Technology, University of Bombay, Matunga, Bombay 400 019, India

(Received 9 September 1993; in revised form 13 April 1995)

Abstract—The technique of gas disengagement is popularly used to assess the bubble size distribution in bubble columns. The technique involves the dynamic measurement of dispersion height when the gas supply is stopped. In this paper a mathematical model has been proposed for the process of dynamic gas disengagement. It has been shown that the initial faster disengagement is due to the presence of internal liquid circulation and not due to the presence of very large bubbles. Further, slower disengagement has been attributed to the transition from heterogeneous dispersion to homogeneous dispersion. The new model also explains the effects of superficial gas velocity, column diameter, column height and liquid phase physical properties on the gas disengagement.

Key Words: dynamic gas disengagement, bubble columns, two bubble class model, bubble rise velocity, liquid circulation velocity

INTRODUCTION

Bubble columns are widely used in the chemical industry as reactors for its simplicity and inexpensive means of contacting gas and liquid. In bubble columns, the size (and shape) of bubbles is the most important parameter. It determines the bubble rise velocity, the gas hold-up, the interfacial area, the residence time of the gas, and the levels of turbulent liquid circulation. The turbulent liquid circulation, in turn, governs the liquid phase mixing and the heat transfer. All these parameters are important in deciding the performance of bubble column reactors. Furthermore, the bubble size can have a significant influence on the product distribution in the case of a complex reaction.

In view of the importance of the knowledge of bubble size distribution, there have been several reports related to this aspect. A host of techniques (such as photographic methods, LDA measurements and hot probe measurements) are available for actual bubble size measurements in sparged reactors and a comprehensive list is given in the review by Joshi *et al.* (1990). However, most of the techniques involve the use of expensive electronics and this may impose a limitation on their use.

Sriram & Mann (1977) presented a very simple technique for getting the bubble size distribution, called the gas disengagement technique (GDT). This technique involves the sudden closure of the gas flow (in the case of batch operation and both liquid and gas in the case of columns operated in a continuous manner) and noting the dynamic response of the dispersion height. The log–normal distribution was found to explain the observed rate of gas disengagement. Under their conditions of operation the bubble size showed a log–normal distribution with a single peak.

Several workers have used the GDT proposed by Sriram & Mann to predict bubble size distribution. Vermeer & Krishna (1981) analyzed the hydrodynamic behaviour of bubble columns operated in the "churn-turbulent" flow regime using the GDT. In addition, the size distribution was also analysed by gas residence time distribution (RTD). The disengagement curves were fitted by two distinct curves. The first one corresponded to the sharply decreasing portion and had a slope equal to the superficial gas velocity V_G. This portion was attributed to the disengagement of the

†To whom all correspondence should be addressed.

large bubbles. The second and less steep part of the curve was attributed to the smaller bubbles entrained by the local liquid circulation. From a combination of GDT and RTD studies, they concluded that, for bubble columns operating in the churn turbulent flow regime, the gas is transported in the form of large and small bubbles. Godbole *et al.* (1982), Kelkar *et al.* (1983) and Shah *et al.* (1985) have investigated the effect of coalescing and non-coalescing nature of dispersion on the rate of gas disengagement. Recently, Schumpe & Grund (1986) have given a very systematic and comprehensive mathematical analysis of GDT including a detailed derivation for a more realistic sparger design.

Most of the above investigators used the disengagement technique as a secondary tool for getting more information about the more important design parameters such as mass and heat transfer coefficients. Further, all these investigators (with the exception of Sriram & Mann, who actually concluded with a unimodal size distribution for $V_G = 0.02$ m/s) *a priori* assumed a bimodal size distribution for the bubble size. Although this description of the gas hold-up by a two bubble class model is able to explain some of the observed rates of mass transfer, it cannot explain the following commonly observed phenomena in bubble columns.

Based on the assumption of two bubble class model, the rise velocities of the large bubbles were found to be of the order of 0.8–1.2 m/s (Schumpe & Grund 1986; Vermeer & Krishna 1981). A bubble rising at a velocity of 1 m/s will be roughly 0.05–0.1 m in diameter, which seems unrealistic in a column of 0.2–0.3 m i.d. and a superficial gas velocity of 0.1–0.2 m/s. Secondly, actual bubble size measurements by various workers using different techniques (Ueyama *et al.* 1980; Lewis & Davidson 1982; Saxena *et al.* 1990; Wilkinson 1991) show a continuous size distribution for the bubble size and not the bimodal distribution assumed by the above-mentioned investigators. Only in the case of highly viscous liquids has the bimodal distribution been observed by actual size measurement.

In the present paper, a model has been proposed for the hold-up structure in bubble columns operated under churn–turbulent regime. The observed GDT curves will be explained on the basis of this model. The first section gives the qualitative description of GDT followed by a mathematical analysis of GDT curve. Subsequently, the model has been used to explain the experimental observations.

QUALITATIVE DESCRIPTION OF GAS DISENGAGEMENT

In this section, the GDT curve is interpreted in the light of flow transition in bubble columns. Two types of flow regimes are encountered in bubble columns. Figure 1(a) and (b) shows schematically homogeneous and heterogeneous regimes, respectively. The homogeneous regime is observed in bubble columns at relatively low superficial gas velocities ($V_G < 0.05$ m/s) and is characterized by a uniform distribution of the gas hold-up. No gradients (radial or axial) are assumed to exist as shown in figure 1(c). The regime is also marked by a weak liquid circulation. In the heterogeneous regime, on the other hand, there is a radial gas hold-up profile as shown in figure 1(d). The liquid is relatively back-mixed and there is an intense recirculation of the liquid phase. This occurs at relatively high superficial gas velocities ($V_G > 0.05$ m/s). The radial gas hold-up profile has been described by a number of workers to be parabolic with a maximum at the center. Because of this local maximum in the gas hold-up, the density of gas-liquid dispersion is less at the center and more near the walls, where the gas hold-up is negligible. This density difference is the driving force for the liquid circulation. Similarly, the liquid circulation generated in the lower part of the column drives the bubbles towards the column center and this sustains the radial gas hold-up profile. Therefore, more gas rushes in the central region and progressively less gas gets sparged as one goes radially towards the wall.

During the gas disengagement, the gas flow is stopped suddenly. Once this is stopped, the liquid flow rate and the radial hold-up profile will start decaying. A schematic representation of the two segments of the GDT curve is shown in figure 2. In the first part of the GDT curve (part A–B), the gradient in radial gas hold-up decays due to the radial dispersion and the profile becomes flat. As the profile decays the intensity of liquid circulation is negligible. Therefore, the first part A–B of the GDT curve corresponds to the transition from heterogeneous to homogeneous regime and

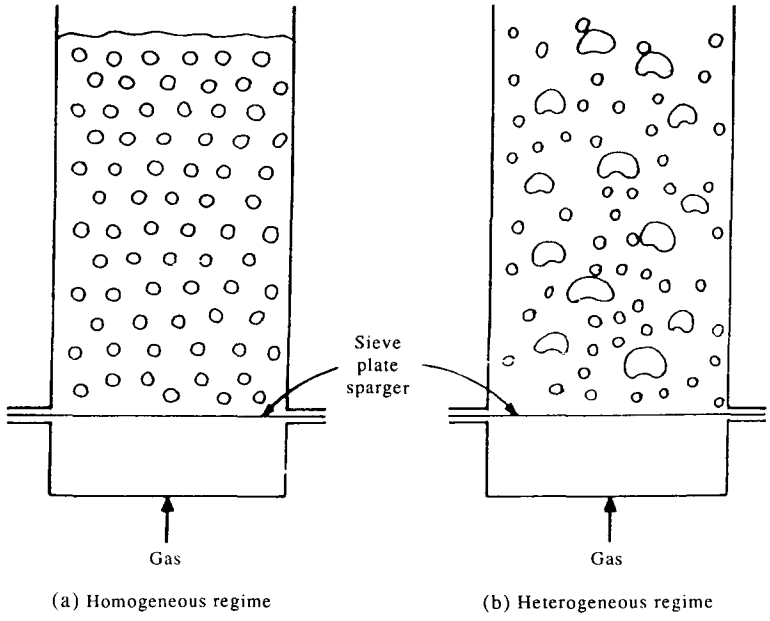

Figure 1(a). Schematic representation of the homogeneous regime.
Figure 1(b). Schematic representation of the heterogeneous regime.

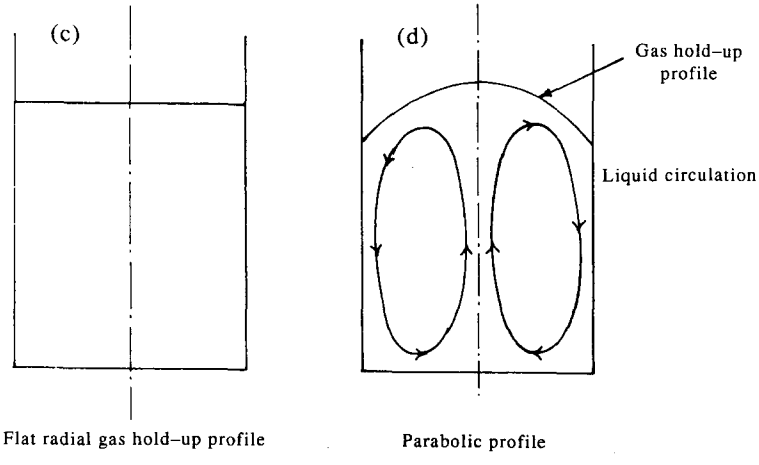

Figure 1(c). Schematic representation of the flat radial gas hold-up profile in the homogeneous regime.
Figure 1(d). Schematic representation of the parabolic radial gas hold-up profile in the heterogeneous regime.

perhaps only partly due to the disengagement of large bubbles. We propose that, in the first part, the spatial configuration of the bubble concentration changes. The second part B–C of the curve corresponds to the disengagement of the homogeneous bubble column. However, during the first part, when the radial dispersion is nullifying the gas hold-up profile, there is a simultaneous disengagement of bubbles.

ANALYSIS OF GAS DISENGAGEMENT CURVE

Decay of the radial profile

As discussed earlier, the initial parabolic gas hold-up profile in a radial direction decays to a flat profile. In this section we present a simple analysis for the time required for the radial hold-up to become practically flat. A one-dimensional dispersion model gives the equation

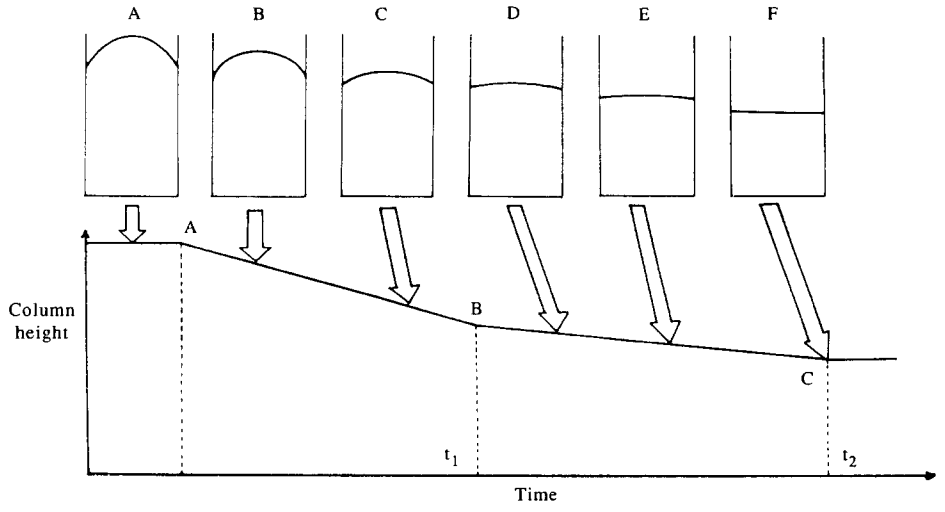

Figure 2. Figure describing dynamic disengagement using the present model.

$$\frac{\partial \epsilon_G}{\partial t} = \frac{1}{r}\frac{\partial}{\partial r}\left(rD_{rG}\frac{\partial \epsilon_G}{\partial r}\right), \tag{1a}$$

where ϵ_G denotes the local fractional gas hold-up, r denotes the radial coordinate, t denotes time and D_{rG} denotes the radial dispersion coefficient. The initial and boundary conditions for the above equations are as follows:

Initially the hold-up profile is parabolic, i.e.

$$\text{at } t = 0, \quad \epsilon_G = 2\bar{\epsilon}_G\left[1 - \left(\frac{r}{R}\right)^2\right], \tag{1b}$$

where $\bar{\epsilon}_G$ is the average fractional gas hold-up and R is the column radius. Also

$$\text{for } t > 0, \quad \text{at } r = 0, \quad \epsilon_G \text{ is not infinite.} \tag{1c}$$

Moreover, there is no dispersive flux across the column wall, i.e.

$$\text{for } t > 0, \quad \text{at } r = R, \quad \frac{\partial \epsilon_G}{\partial r} = 0. \tag{1d}$$

If we assume that the dispersion coefficient of the gas phase remains unchanged, [1a] can be written in the following dimensionless form:

$$\frac{\partial \epsilon_G}{\partial \tau} = \frac{1}{\eta}\frac{\partial}{\partial \eta}\left(\eta\frac{\partial \epsilon_G}{\partial \eta}\right), \tag{2}$$

where

$$\tau = \frac{tD_{rG}}{R^2} \quad \text{and} \quad \eta = \frac{r}{R}, \tag{3}$$

where τ is dimensionless time and η is dimensionless radius. Now, at $\tau = \infty$, ϵ_G will attain a steady state value $\bar{\epsilon}_G$, for all values of r. Therefore, we seek the solution of the form

$$\epsilon_G(\eta, \tau) = \bar{\epsilon}_G - \epsilon_{Gt}(\eta, \tau). \tag{4}$$

Thus we split the solution into a steady state limiting part, $\bar{\epsilon}_G$ and a transient function ϵ_{Gt}. Using [4], [2] becomes

$$\frac{\partial \epsilon_{Gt}}{\partial \tau} = \frac{1}{\eta}\frac{\partial}{\partial \eta}\left(\eta \frac{\partial \epsilon_{Gt}}{\partial \eta}\right), \qquad [5]$$

We seek a solution of [5] of the form

$$\epsilon_{Gt} = Z(\eta)T(\tau), \qquad [6]$$

where Z is a function of η alone and T is a function of τ alone. Substituting [6] in [5] and solving the resulting two differential equations with the initial and boundary conditions [1b]–[1d], we get

$$\epsilon_G(\eta, \tau) = \bar{\epsilon}_G - 8\bar{\epsilon}_G \sum_{n=1}^{\infty} \frac{J_0(\alpha_n \eta)}{\alpha_n^2 J_0(\alpha_n)} \exp(-\alpha_n^2 \tau), \qquad [7]$$

where, $\alpha_n = 3.832,\ 7.016,\ 10.173, \ldots,$ for $n = 1, 2, 3, \ldots, \infty$, are the roots of $J_1(\alpha) = 0$, and J_0 and J_1 are Bessel's functions of zero-th and first order, respectively. Equation [7] describes the decay of the initial parabolic hold-up profile to the final flat profile at $\tau = \infty$, with intermediate profiles between $\tau = 0$ and $\tau = \infty$. Now, consider the location $r = 0$. At this position, initially the hold-up will be $2\bar{\epsilon}_G$ and finally at $(t = \infty)$ it will become $\bar{\epsilon}_G$. The time required for the hold-up at $r = 0$ to reach its final steady state value $\bar{\epsilon}_G$, within 99.95%, denoted by t_1, can be obtained from [7] as

$$\tau_1 = 0.6 \quad \text{or} \quad t_1 = \frac{0.6R^2}{D_{rG}}. \qquad [8]$$

The value t_1 in [8] can be taken to indicate the time required for the initial parabolic hold-up profile to become practically flat (the centreline value of hold-up reaching a value within 99.95% of the final steady state value).

MASS BALANCE DURING DISENGAGEMENT

In this section a simple mass balance is presented during the disengagement of the gas. Let the superficial gas velocity before disengagement be V_G and the average fractional gas hold-up be $\bar{\epsilon}_G$. Let the dispersion height during the steady state operation be h_2 and let h_0 be the clear liquid height. During disengagement, let the instantaneous superficial gas velocity and gas hold-up be V_G^* and $\bar{\epsilon}_G^*$, respectively. Let h be the instantaneous dispersion height. Taking gas phase material balance,

$$\text{Gas leaving the column} = V_G^* A \rho_G, \qquad [9]$$

$$\text{Rate of accumulation of gas} = -\frac{d}{dt}(\bar{\epsilon}_G^* h A \rho_G). \qquad [10]$$

Equating [9] and [10] we get

$$-\frac{d}{dt}(\bar{\epsilon}_G^* h) = V_G^*. \qquad [11]$$

The instantaneous gas hold-up ϵ_G^* is given by

$$\bar{\epsilon}_G^* = \frac{h - h_0}{h}. \qquad [12]$$

Combining [11] and [12] we get

$$-\frac{dh}{dt} = V_G^*. \qquad [13]$$

The instantaneous gas superficial gas velocity V_G^* in the heterogeneous regime can be written using the modified drift flux model of Joshi *et al.* (1990),

$$\frac{V_G}{\epsilon_G} = C_0 V_G + C_1, \quad [14]$$

where C_0 and C_1 are the constants given by

$$C_0 = \frac{\langle \epsilon_G V_G \rangle}{\langle \epsilon_G \rangle \langle V_G \rangle} + \frac{\langle \epsilon_G V_A \rangle}{\langle \epsilon_G \rangle}, \quad [15]$$

$$C_1 = \frac{\langle \epsilon_G \epsilon_L V_S \rangle}{\langle \epsilon_G \rangle}, \quad [16]$$

where the quantities enclosed in $\langle\rangle$ represent the averages. The contribution of liquid circulation velocity V_A is not considered in the standard drift flux model. However, the modified drift flux model incorporates the effect of liquid circulation velocity V_A on the constant C_0 in [15]. A combination of [13] and [14] gives the instantaneous dispersion height as a function of time and describes the GDT curves in the heterogeneous regime:

$$C_1 t = h_0 \ln\left(\frac{h_2 - h_0}{h - h_0}\right) + (1 - C_0)(h_2 - h), \quad [17]$$

where h_2 is the dispersion height at steady state condition before disengagement, h_0 is the clear liquid height and h is the instantaneous dispersion height at time t. Equation [17] is valid only for $t \leqslant t_1$, i.e. up to the time when the radial profile flattens out.

RESULTS AND DISCUSSIONS

In this section, we present results of our mathematical model described in the earlier section. The time at which the GDT graph changes slope is taken as the experimental value of t_1 (figure 2). The value of t_1 is predicted using [8]. The gas phase dispersion coefficient in [8] is evaluated as

$$D_{rG} = lu', \quad [18]$$

where l is the length scale of turbulence and u' is the RMS velocity. Joshi (1980) has proposed the following relation for the length scale in the heterogeneous regime:

$$l = 0.08\, D, \quad [19]$$

where D is the column diameter. The RMS velocity can be written in terms of power dissipation per unit mass E and the length scale as

$$u' = (lE)^{1/3}. \quad [20]$$

Joshi (1980) also proposed following relation on the basis of energy balance to predict the RMS velocity:

$$E = g(V_G - \epsilon_G V_S), \quad [21]$$

where V_S is the slip velocity. Combining [18], [19], [20] and [21], D_{rG} can be written as

$$D_{rG} = [g(V_G - \epsilon_G V_S)(0.08D)^4]^{1/3}. \quad [22]$$

In [22], V_S was obtained in each case using the drift-flux model. The same model has been shown to explain the pressure drop and heat transfer coefficients in the bubble columns.

The comparison of model prediction of t_1 (using [8]) with the experimental data of Schumpe & Grund (1986), Kelkar *et al.* (1983), Godbole *et al.* (1982) and Vermeer & Krishna (1981) is given in table 1(A)–(D), respectively.

The comparison in table 1(A) is fairly good. In table 1(B), for the second data point, which is at a lower V_G than the first data point, the experimental value of t_1 is lower. This is not consistent with the experimental trend observed by other workers. However, for all the remaining datapoints, the comparison with the experimental data is reasonable. In the case of table 1(C) and (D), the comparison with the experimental data, though not so good quantitatively (average error = 27%, maximum error = 40%), shows qualitatively correct trends, i.e. the time t_1 increases with a decrease

Table 1(A). Experimental data on gas disengagement (data of Schumpe & Grund 1986), air–water system, ring distributor type sparger, $h_0 = 3.1$ m, $D = 0.3$ m

Superficial gas velocity (m/s)	Gas hold-up (—)	t_l experimental (s)	t_l predicted (s)
0.1695	0.255	2.4	2.26
0.0873	0.182	3.5	3.36

Table 1(B). Experimental data on gas disengagement (data of Kelkar *et al.* 1983), air–0.5% methanol system, $D = 0.3$ m

Superficial gas velocity (m/s)	Gas hold-up (—)	t_l experimental (s)	t_l predicted (s)
0.147	0.35	2.4	2.49
0.096	0.28	2.2	3.13
0.02	0.07	4.0	5.01

Table 1(C). Experimental data on gas disengagement (data of Godbole *et al.* 1982), air–20% glycerine solution, $D = 0.305$ m

Superficial gas velocity (m/s)	Gas hold-up (—)	t_l experimental (s)	t_l predicted (s)
0.2398	0.27	2.6	1.76
0.1982	0.25	2.7	1.92
0.0798	0.16	3.0	2.96
0.0368	0.12	3.2	5.30

Table 1(D). Experimental data on gas disengagement (data of Vermeer & Krishna 1981), N_2–turpentine-5, $D = 0.19$ m

Superficial gas velocity (m/s)	Gas hold-up (—)	t_l experimental (s)	t_l predicted (s)
0.281	0.41	2.2	1.42
0.189	0.32	2.5	1.67
0.103	0.26	3.0	2.53

in the superficial gas velocity. It should be noted that the same prescription for the dispersion coefficient was used in all the cases (using [22]) for the prediction of t_l.

The trend observed in table 1 can be explained qualitatively as follows. In the heterogeneous regime, as the gas velocity increases, the radial profile develops and becomes more steep. As against this, the dispersion coefficient also increases and tries to nullify the radial hold-up profile. This increase in the dispersion coefficient is, however, not very strong compared with the increase in the hold-up profile. This leads to an increase in the time required for the radial profile to decay once the disengagement begins.

Table 1(D) shows values of t_l for an N_2–turpentine system. The viscosity of turpentine is very much less than that of water and therefore the dampening force for evening out the radial profile is less, compared with that of a water system. This is clearly evident from table 1(D), where t_l is substantially higher than t_l for an air–water system.

Liquid circulation velocity

Some of the previous workers (Schumpe & Grund 1986; Vermeer & Krishna 1981) have obtained the values of rise velocities of large bubbles on the basis of two bubble class models applied to the GDT data. The values of rise velocities for the large bubbles are greater than 1 m/s, even for air–water systems. These values appear to be unrealistically large. It appears that the large values of rise velocities are due to the high values of liquid circulation velocities. To check the validity of this hypothesis, it was though desirable to compare the experimental and predicted values of liquid circulation velocities. Experimental values of the liquid circulation velocity have been compiled by Joshi (1980). The predicted velocity was obtained by the following procedure.

The riser–downcomer model proposed by Ranade & Joshi (1987) divides the bubble column (excluding the sparger dominated region and the top coalescing region of the column) into two regions. The liquid flows in the upward direction through the central region (riser) and comes down through the region near the wall (figure 3). The result of this analysis is that

$$\frac{V_G}{\epsilon_G} = V_S + \frac{KV_A}{D^{1/3}}. \qquad [23]$$

Equation [23] predicts ϵ_G to be independent of the column diameter. The value of the constant K is zero in the homogeneous regime, which corresponds to the feeble liquid circulation, and will gradually increase in the heterogeneous regime. At higher gas velocities, K will asymptotically approach a constant value. Comparison of [14] and [23] gives the following relationship between the riser–downcomer model and the drift-flux model:

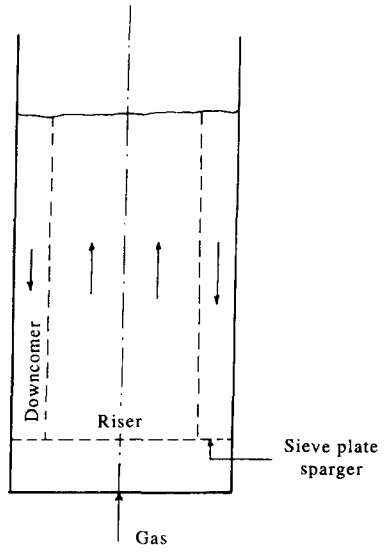

Figure 3. Schematic representation of the riser–downcomer model.

$$C_0 = \frac{KV_A}{V_G D^{1/3}}. \qquad [24]$$

The liquid circulation velocity was predicted using [24], with the value of C_0 obtained using the drift-flux plot (figure 4) and the value of K reported by Ranade & Joshi (1987).

Table 2 gives the experimental and predicted liquid circulation velocities for various values of the superficial gas velocities from the data of Schumpe & Grund (1986). It can be seen from table 2 that the contribution of the liquid circulation velocities to the rise velocities of large bubbles is substantial. If the contribution of the liquid circulation velocity is removed from the bubble rise velocities, we may get realistic values of the bubble rise velocities.

Prediction of DGD curve

Equation [17], which was based on simple mass balance, was used to predict the height as a function of time for the steep portion of the GDT curve (for $t < t_1$). The data of Schumpe & Grund (1986) were used for this purpose. The constants C_0 and C_1 in the drift-flux model in [14] were

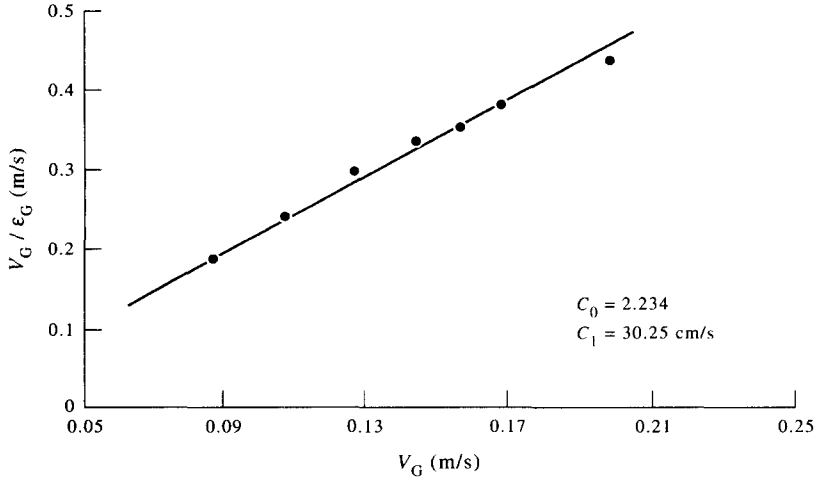

Figure 4. Drift-flux model for Schumpe & Grund data.

Table 2. Comparison of liquid circulation velocities (data of Schumpe & Grund 1986)

Superficial gas velocity (m/s)	Total gas hold-up (—)	Liquid circulation velocity	
		Experimental (m/s)	Predicted (m/s)
0.075	0.196	0.45	0.46
0.100	0.184	0.59	0.51
0.125	0.208	0.67	0.58
0.150	0.227	0.73	0.65
0.175	0.250	0.78	0.74
0.200	0.265	0.83	0.80

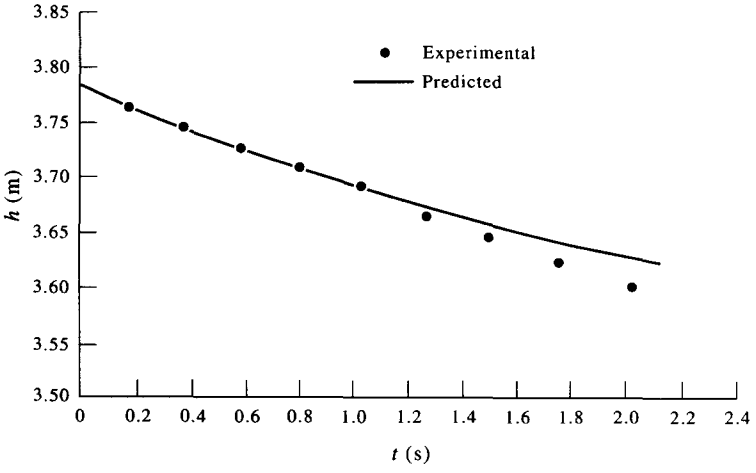

Figure 5. Disengagement curve predicted by the present model.

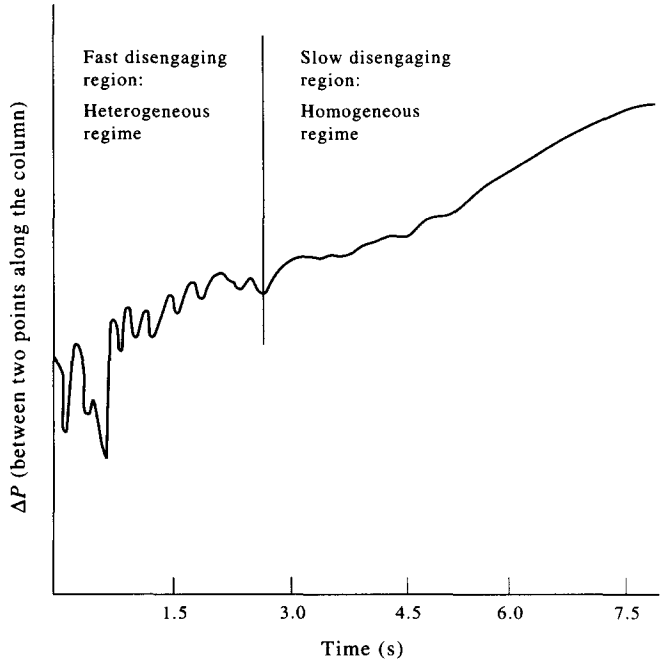

Figure 6. Typical differential pressure profile obtained after sudden shutdown in gas supply, adapted from Shetty *et al.* (1992).

obtained from the drift-flux plot form. Figure 5 shows the disengagement curve constructed from [17] for one superficial gas velocity of Schumpe & Grund data. The figure shows a favourable agreement with the GDT curve obtained experimentally.

Some additional evidence for the validity of the present model can be obtained from a recent publication (Shetty *et al.* 1992). The authors have made intelligent use of pressure probe to record the pressure fluctuations during the dynamic gas disengagement. A typical record of pressure fluctuations during the dynamic gas disengagement is shown in figure 6. From the measurements it can be seen that the flow is highly turbulent during the first part (line AB in figure 2) and relatively much less turbulent in the second part (line BC in figure 2) of the dynamic gas disengagement. These are known to be the characteristic features of heterogeneous and homogeneous regimes, respectively. The technique of gas disengagement is a very powerful tool for the elucidation of flow patterns in multiphase reactors such as gas–liquid bubble columns, fluidized beds, three-phase slurry reactors, liquid–gas and liquid–liquid spray columns. The GDT measurements can be used to measure the relative velocities of the dispersed bubbles or drops or particles, depending upon the multiphase system. The real relative velocities are known to be markedly different from the terminal velocities and these are lower (hindered) in the homogeneous regime and can be higher in the heterogeneous regime.

The GDT technique can measure the size distribution of the dispersed phase. It may be emphasized that the size and velocity distribution of the dispersed phase (bubbles, drops and particles) forms very basic information for the design of multiphase reactors and can be obtained from simple disengagement experiment.

CONCLUSIONS

(1) The observed gas disengagement technique (GDT) curve has been satisfactorily explained by a single bubble class model. The predicted values of t_1 show good qualitative agreement with the experimental data. All the observed peculiarities associated with the GDT curve have been accounted for.

(2) Unrealistically high values of the bubble rise velocities obtained from GDT data have been reinterpreted in view of the contribution from the liquid circulation velocities.

(3) There is always a possibility of some bubble size distribution. However, the actual distribution is unlikely to be as wide as given by the two bubble class models.

(4) A simple model based on material balance was used to predict the shape of the GDT curve in the steep region. The comparison was reasonable.

Acknowledgement—This research work was supported by a grant under the Indo-US Collaborative Research Program (USHRF/92/33t).

REFERENCES

Godbole, S. P., Honath, M. F. & Shah, Y. T. 1982 Holdup structure in highly viscous newtonian and non-newtonian liquids in bubble columns. *Chem. Engng Commun.* **16,** 119–134.

Godbole, S. P., Joseph, S., Shah, Y. T. & Carr, N. L. 1984 Hydrodynamics and mass transfer in a bubble column with an organic liquid. *Can. J. Chem. Engng* **62,** 440–445.

Joshi, J. B., 1980 Axial mixing in multiphase contactors–a unified correlation. *Trans. Inst. Chem. Engng* **58,** 155–165.

Joshi, J. B., Patil, T. A. & Ranade, V. V. 1990 Measurement of hydrodynamic parameters in three phase sparged reactors. *Rev. Chem. Engng* **6,** 74–227.

Joshi, J. B., Ranade, V. V., Gharat, S. D. & Lele, S. S. 1990 Sparged loop reactors. *Can. J. Chem. Engng* **68,** 705–742.

Kelkar, B. G., Godbole, S. P., Honath, M. F., Shah, Y. T., Carr, N. L. & Deckwer, W.-D. 1983 Effect of addition of alcohols on gas holdup and backmixing in bubble columns. *AIChE Jl* **29,** 361–369.

Krishna, R., Wilkinson, P. M. & van Dierendonck, L. L. 1991 A model for gas holdup in bubble columns incorporating the influence of gas density on flow regime transition. *Chem. Engng Sci.* **46,** 2491–2495.

Lewis, D. A. & Davidson, J. F. 1982 Bubble splitting in shear flow. *Trans. Inst. Chem. Engrs* **60,** 283–292.

Ranade, V. V. & Joshi, J. B. 1987 Momentum, mass and heat transfer in bubble column reactors. In *Transfer Processes in Multiphase Systems* (Edited by Upadhyay, S. N.), p. 113. Banaras Hindu University Press, India.

Saxena, A. C., Rao, N. S. & Saxena, S. C. 1990 Bubble size distribution in bubble columns. *Can. J. Chem. Engng* **68,** 159–161.

Schumpe, A. & Grund, G. 1986 The gas disengagement technique for studying gas holdup structure in bubble column. *Can. J. Chem. Engng* **64,** 891–896.

Shah, Y. T., Joseph, S., Smith, D. N. & Ruether, J. A. 1985 Two bubble class model for churn-turbulent bubble column reactor. *Ind. Engng Chem. Proc. Des. Dev.* **24,** 1096–1104.

Shetty, S. A., Kantak, M. V. & Kelkar, B. G. 1992 Gas-phase backmixing in bubble column reactors. *AIChE Jl* **38,** 1013–1026.

Sriram, K. & Mann, R. 1977 Dynamic gas disengagement: a new technique for assessing the behaviour of bubble columns. *Chem. Engng Sci.* **32,** 571–580.

Ueyama, K., Morooka, S., Koide, K., Kaji, H. & Miyauchi, T. 1980 Behaviour of gas bubbles in bubble columns. *Ind. Engng Chem. Proc. Des. Dev.* **19,** 592–599.

Vermeer, D. J. & Krishna, R. 1981 Hydrodynamics and mass transfer in bubble columns operating in the churn-turbulent regime. *Ind. Engng Chem. Proc. Des. Dev.* **20,** 475–482.

Wilkinson, P. M. 1991 Physical aspects and scale-up of high pressure bubble columns. Ph. D. thesis, University of Groningen, The Netherlands.

Zuber, N. & Findlay, J. A. 1965 Averaging volumetric concentration in two phase systems. *ASME J. Heat Transfer* **87,** 453–468.